Doping assisted floating zone crystal growth of decompositional compounds

Takaho Tanaka
Scientific Information Office, National Institute for Materials Science
E-mail: TANAKA.Takaho@nims.go.jp

Abstract. This article describes floating zone (FZ) crystal growth of decompositional compounds, which is assisted by addition of an extra element to constituent elements. Examples are; FZ crystal growths of WC assisted by B addition and YB_{50} and ScB_{19} assisted by Si addition. All they decompose without melting as temperature increased. The addition of the extra element enables the compounds to melt by reducing melting temperature and stabilizing the compound phase.

1. Introduction

Materials science has always demanded new compounds that may have novel chemical, physical and functional properties with potential applications. Nowadays main stream of materials science is nano-related investigations. Growth of bulk single crystals seems to be an old fashioned investigation. Nanomaterials science could supply variety of nanoforms of element or known compounds, such as fullerene, naotubes and nanowires, however, it could supply little new compounds. Search of new compounds is still an important materials science research field, and if one can obtain a single crystal of such new compounds, it would be very beneficial for the investigation of the compound. Among many crystal growth techniques floating zone (FZ) technique, which is one of zone melting (ZM) crystal growth methods, is one of most powerful tools for growing a single crystal of high melting temperature compounds. FZ technique enables crucibleless growth of crystals, thus the obtained crystal is free from contamination by a crucible material. Obviously FZ growth requests compounds to melt. Compounds that decompose without melting as temperature increased are out-of-target of FZ technique. This manuscript describes a method growing a single crystal of some types of decompositional compounds, where the addition of an extra element plays a key role for successful FZ crystal growth of such compounds.

2. Floating zone method

Here I describe briefly an example of a floating zone equipment that I have used. Figure 1 shows schematic drawing of the system. It is an image furnace using 4 pairs of a Xenon lamp and an ellipsoidal mirror, which are diagonally arranged to achieve uniform temperature distribution along circumference of the growing crystal. Raising heating power increases the temperature at the focus point of the Xenon lamp image, consequently the molten zone is formed. Once the molten zone is formed, a raw polycrystalline rod is fed into the upper part of the molten zone and a single crystal grows from the bottom part of the molten zone by driving synchronously

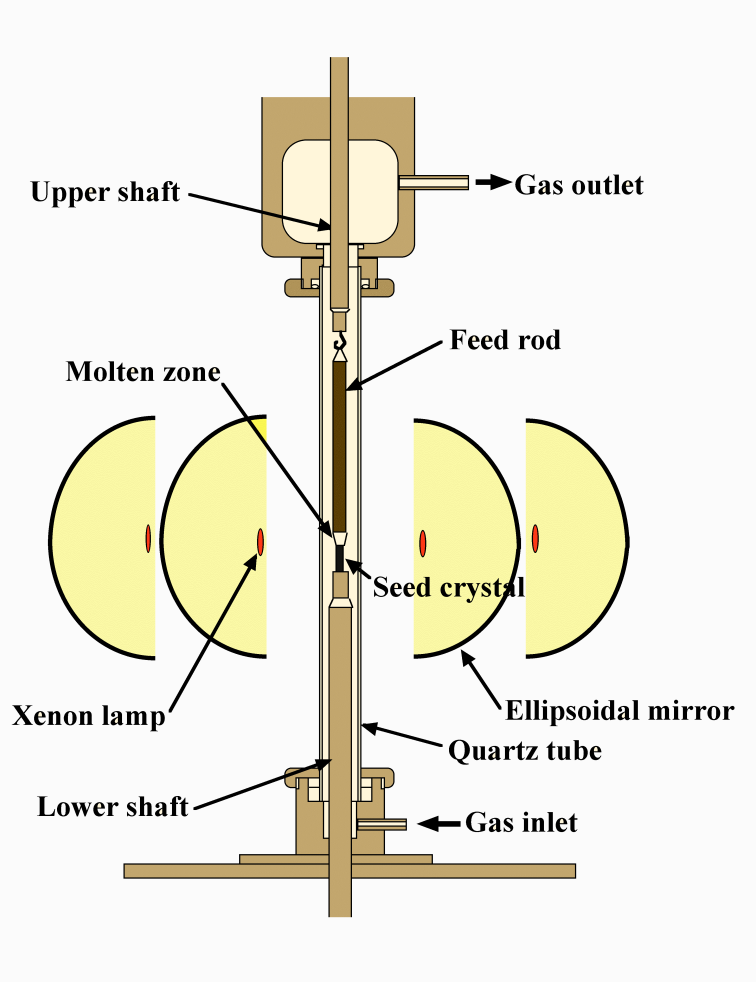

Figure 1. Schematic drawing of a 4 Xenon lamp-ellipsoidal mirror image furnace.

both the upper and lower shafts downwards. Differential drive of the upper and lower shafts is also often used to control diameter of the growing crystal. The upper and lower shafts used to be counter-rotated to make uniform both composition and temperature in the molten zone. Halogen lamp is often used as heat source instead of Xenon lamp. Halogen lamp is useful for materials with melting temperatures up to about 2000 °C. Xenon lamp can melt higher melting temperature materials than halogen lamp up to about 2500 °C. Radio frequency induction heating is almost only one heating method to melt materials with melting temperature higher than 2500 °C. Heating power control is essential to grow a high quality single crystal. Heating power deficiency may freeze a molten zone and excess heating power may drop the molten zone increasing its volume too much.

For FZ crystal growth of compounds, investigation of phase diagram of the compound is essential to know what melting behavior the compound has. Typically melt growth methods such as FZ and Czochralski (CZ) methods are applied to a congruent melting composition, however FZ is applicable to grow a crystal from a molten zone whose composition is different from that of the crystal, if both the crystal and melt can coexist under equilibrium. A part of the phase diagram of a compound A_mB_n is shown in figure 2 as an example, where congruently melting composition is assumed to coincide to the stoichiometric composition. The compound

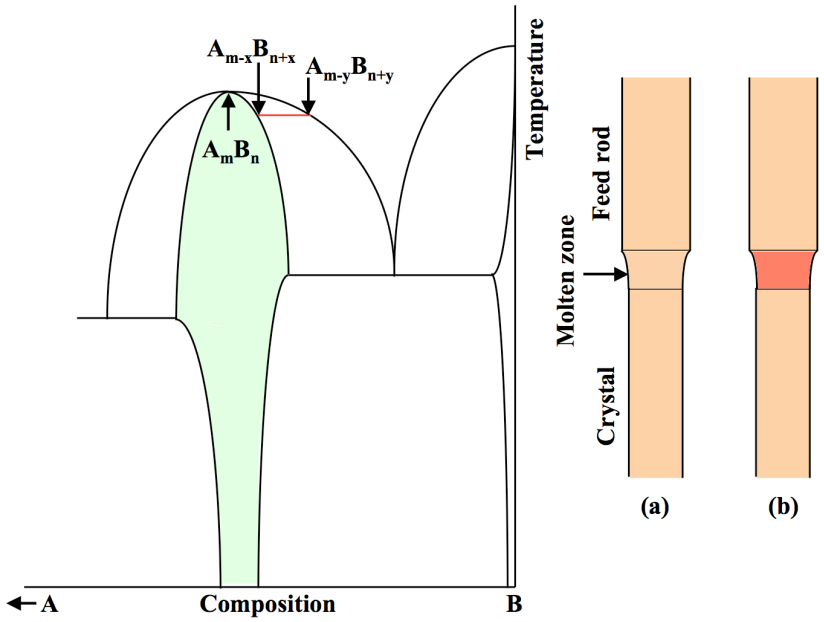

Figure 2. Examples of growing single crystals with (a) the congruent composition A_mB_n, and (b) an incongruent composition $A_{m-x}B_{n+X}$.

A_mB_n has a nonstoichiometric and variantly melting region that is indicated by light green. It is rather easy to grow a single crystal with the congruent composition of A_mB_n. As shown in mode (a), compositions of all the feed rod, molten zone and growing crystal should coincide to A_mB_n. On the other hand, to grow a single crystal with a nonstoichiometric composition of $A_{m-x}B_{n+x}$, compositions of both the feed rod and growing crystal should be $A_{m-x}B_{n+x}$ and the molten zone should have a composition of $A_{m-y}B_{n+y}$ that equilibriumly coexists with $A_{m-x}B_{n+x}$, which is indicated in the phase diagram. This growth mode is shown in (b), where the feed rod with the composition of $A_{m-x}B_{n+x}$ melts in at the top of the molten zone with the composition of $A_{m-y}B_{n+y}$ and the crystal with the composition of $A_{m-x}B_{n+x}$ steadily grows from the bottom of the molten zone. Amounts of feed and grow of the material must be balanced to maintain the steady growth condition.

Another example is crystal growth of decompositional compounds. Figure 3 shows a part of the phase diagram of a compound A_mB_n that peritectically decomposes into a melt whose composition is indicated by a green arrow and another higher melting temperature compound AB at elevated temperature. FZ technique allows crystal growth of A_mB_n using a molten zone whose composition is $A_{m-x}B_{n+x}$, for example, as indicated in the figure. This growth mode is often called as self-flux FZ crystal growth. Some fluctuational variation of the molten zone composition does not affect the growth of A_mB_n, which is different from the case of the variantly melting compound as indicated in figure 2(b) where fluctuational variation of the molten zone composition immediately causes a fluctuational variation of the composition of the growing crystal.

In both cases shown in figures 2 and 3, target compounds still coexist equilibriumly with melt phases within some temperature region. Hereafter I will introduce FZ crystal growth of

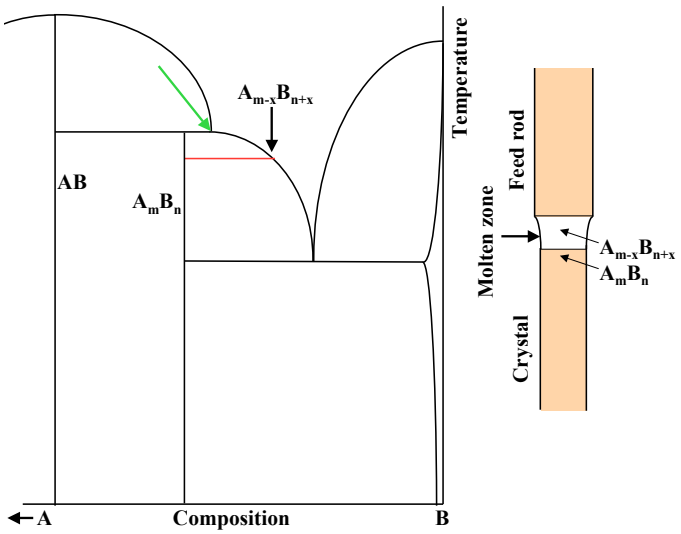

Figure 3. Example of growing a single crystal with the composition A_mB_n that peritectically decomposes into a melt whose composition is indicated by a green arrow and another higher melting temperature compound AB at the peritectic temperature.

compounds that themselves decompose without melting at elevated temperatures and cannot coexist with any melt phases, in which addition of an extra element to constituent elements enables the target compounds coexisting with a melt phase and FZ crystal growth applicable.

3. Tungsten carbide (WC)

WC is one of the most useful cemented carbides because of its hardness, wear resistance and bending strength and is used most widely as a base material of super hard cutting tools. WC has a hexagonal crystal structure with space group $P\bar{6}m2$ (No. 187) and lattice constants a=0.2906 nm and c=0.2837 nm. Basic physical properties have been investigated using sintered polycrystalline bodies till about 1990 because of difficulty of growing single crystals. WC crystals with mm size can be grown by flux growth method using transition metals such as Fe, Co and Ni. Occasionally cm-size crystals have been obtained during industrial synthesis of WC reducing tungsten ore by carbon with metal flux. Such industrial synthesis uses ton-level raw materials so that temperature of the total system very slowly decreases after the reaction, which enables cm-size crystals to grow in the metal flux. However, such crystals have not been popularly available. Here I describe intentional growth of WC crystals using FZ method.

3.1. Phase analysis

It is important to know whether or not WC melts before to start FZ growth experiment as described above. As shown in figure 4 two types of phase diagrams have been available [1, 2]. Both phase diagrams show that there are 3 binary phases of hexagonal W_2C, cubic WC_{1-x} and hexagonal WC. The cubic-WC_{1-x} is a high temperature phase and is stable only above about 2500 °C.

Rudy's phase diagram indicates that WC melts peritecitically above 2776 °C [1]. Then, the floating zone method is applicable to grow WC single crystals using the molten zone with

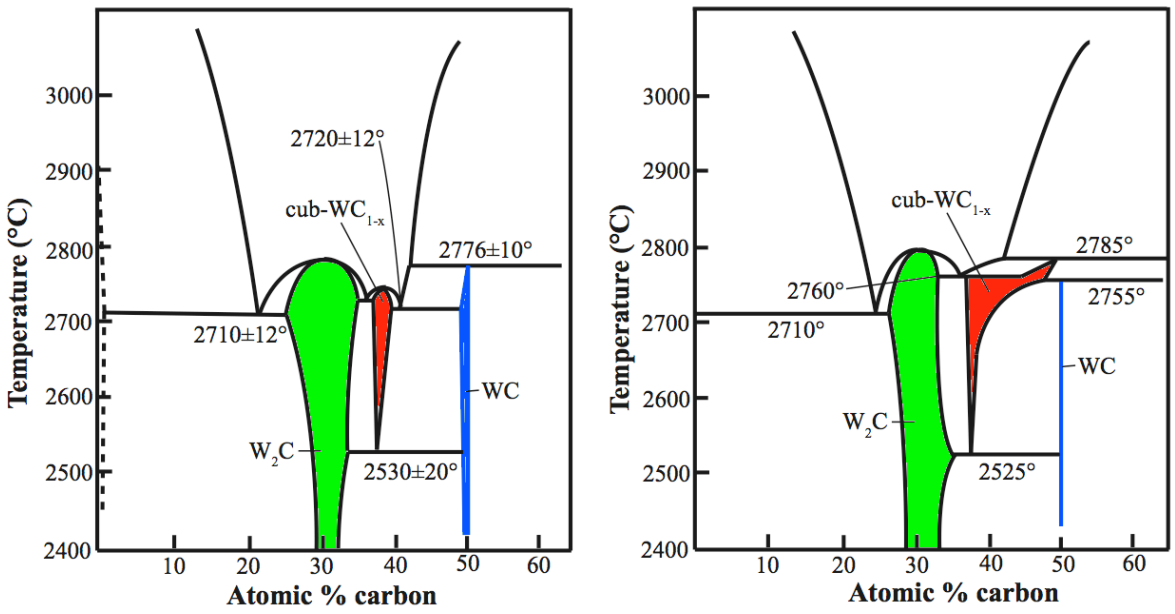

Figure 4. Phase diagrams of W-C binary system. The left one indicates that WC decomposes peritectically at $\sim$ 2776 °C [1]. On the other hand, the right one indicates that decomposition of WC is eutectoid at 2755 °C [2].

peritectic composition. On the other hand, Sara's phase diagram indicates that WC decomposes eutectoid into cubic WC_{1-x} and graphite above 2755 °C [2], which means that the floating zone method is not applicable. Expecting the correctness of the former phase diagram I have tried floating zone crystal growth of WC using a polycrystalline WC rod without adjusting initial molten zone composition. Even the case, after the zone pass with several times of the zone length a WC crystal should start growing although initially graphite grows from the molten zone. However, the obtained zone-passed rod consisted of 3 phases of WC, W_2C and graphite. The result not only simply contradicts with the expectation, but also suggests that there occurred some phase transition/reaction during the zone pass because only two phases are allowed to coexist under an equilibrium condition of binary system. The result revealed that WC does not melt peritectically, and suggested that cubic WC_{1-x} may grow from the molten zone because it decomposes into W_2C and WC when temperatures decrease.

To investigate further what phase transformation/reaction proceeds during the floating zone pass of WC rod we performed a quench experiment instantly shutting down heating power. Temperature of the molten zone region decreased below 1000 °C within several seconds. The quenched rod with $\sim$10 mm diameter was longitudinally cut parallel to the growth axis and the cut surface was polished. The longitudinal section around the molten zone is shown in figure 5(a). The zone-passed rod appeared relatively dense and uniform in the range of $\sim$2 mm from the growth interface, then became a course structure with visible grains beyond the range as shown in the figure. We performed X-ray diffraction analysis for every labeled portion in the figure. The results are shown in figure 5(b). At portion 1, the rod consisted of cubic WC_{1-x} and C (graphite). At portion 2, where temperature is lower than that at portion 1 on leaving the molten zone, most of cubic WC_{1-x} diminished and large amount of W_2C appeared in addition to C, and small amount of WC also appeared. With further decrease of temperature, at portion 3, cubic WC_{1-x} completely diminished and considerable amount of WC was formed. Finally

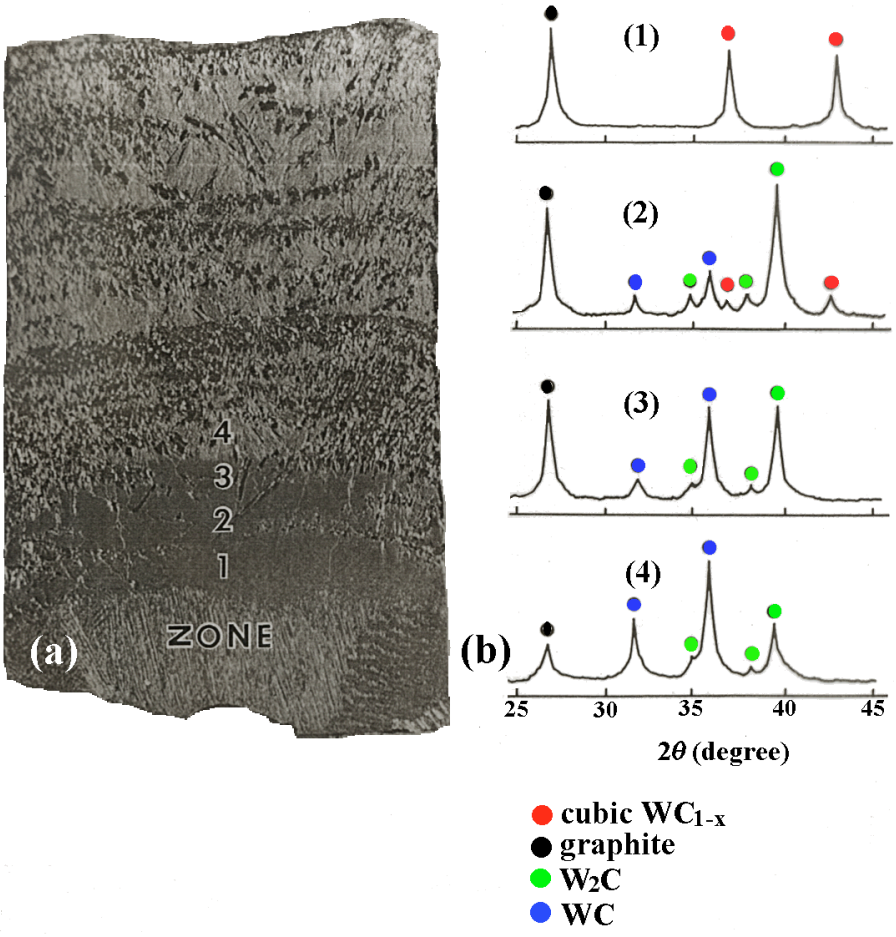

Figure 5. (a) Longitudinal section around the zone quenched during the zone pass of WC rod. (b) X-ray diffraction patterns for every portion labeled in (a). (red) cubic WC_{1-x}, (black) graphite, (green) W_2C and (blue) WC

at portion 4, WC became dominant with small amounts of W_2C and C. These results indicate that the phases growing from the molten zone are cubic WC_{1-x} and xC because sum of both elements must be WC. As temperature decreases on leaving the molten zone, WC_{1-x} kinetically decomposes into W_2C and C. Meanwhile the temperatures of portions 2 and 3 are high enough for forming WC by the reaction between W_2C and C, thus WC gradually increases. However, temperature at portion 4 becomes too low for completing the reaction, thus the zone-passed rod consists of 3 phases of WC, W_2C and C. Sara's phase diagram is more consistent to our result than Rudy's one. Note that more recent phase diagrams reported [3, 4] are inconsistent to our result because they also reported that WC peritectically melts.

3.2. Addition of third element

The fact that WC does not melt peritectically and cannot coexist with melt phase does not allow us FZ crystal growth of WC within the binary W-C phase range. Additional innovative method is necessary to overcome this situation. According to Sara's phase diagram, because it is more consistent to our experimental result, WC decomposes at 2755 °C. The temperature range where cubic WC_{1-x} coexists with the liquid phases is from 2760 to 2785 °C, which is

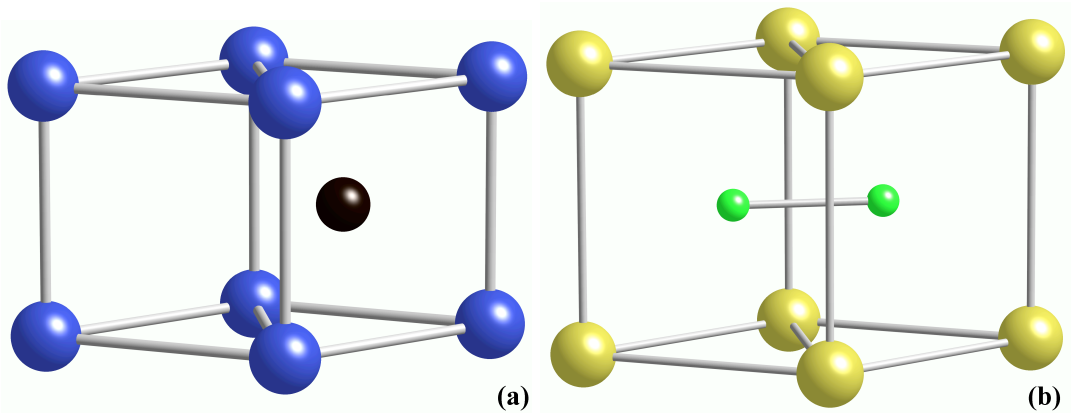

Figure 6. Crystal structures of (a) WC, where large blue spheres are W atoms and a small black sphere is C atom, and (b) MB_2, where large yellow spheres are M atoms and small green spheres are B atoms. WC includes only one C atom in the unit cell, that occupies the center of one of pyramids formed by W atoms. MB_2 includes two B atoms in the unit cell, that occupy the center of both pyramids formed by M atoms.

very narrow. We can expect that a slight addition of a third element may change the mutual phase relation between WC and cubic WC_{1-x}, which allows WC to coexist with melt phase instead of WC_{1-x}. To realize such expectation we should search the third element on the basis of the following four conditions: (1) the third element should form compound with W, (2) the crystal structure of the compound formed between W and the third element should resemble the WC structure, (3) the compound should be stable at sufficiently high temperatures, and (4) the melting behavior of the compound should be suitable to FZ crystal growth.

On the basis of the above 4 criteria we recognized that boron should be the first choice because both WC and transition metal diborides MB_2 (M = Ti, Zr, Hf, Nb, Ta, etc.) show close structural and property similarities, i.e., both have hexagonal crystal structures in which metal and nonmetal hexagonal network layers alternatively stack along the *c*-axis as shown in figures 6a and b, and are refractory materials stable up to 2500 °C. Most of MB_2 melt congruently. Phase diagram of binary W-B system is shown in figure 7 [5], where WB_2 melts congruently at 2365 °C for composition of $WB_{\sim 2.3}$, although the crystal structure of WB_2 is modified from the MB_2-type structure that is shown in figure 6b with including a staggered B layer. Thus B addition may improve WC melting behavior to that FZ crystal growth applicable.

The above expectation was readily verified experimentally by the float zoning of a WC rod with 6 mol% boron. Some single phase has started depositing from the molten zone after about $4 \sim 5$ mm zone travel. X-ray diffraction analysis verified the single phase to be WC, although a very small amount of free carbon was also detected. Electron probe microanalysis indicated that the boron content in the WC phase was less than 0.05 wt% and that in the zone was of the order of 0.5 wt%.

3.3. Floating zone crystal growth

The boron addition enables floating zone crystal growth of WC, however, the zone pass is much more different from that for congruent melting compounds. Composition of molten zone is different from that of growing crystal. Composition relation between the growing crystal, the molten zone and the feed rod is shown in figure 8. The obtained crystal has a nearly stoichiometric composition except for $\sim$ 0.1 at% boron replacing carbon. Meanwhile molten zone composition is much carbon less and boron more from the crystal composition, i.e., W :

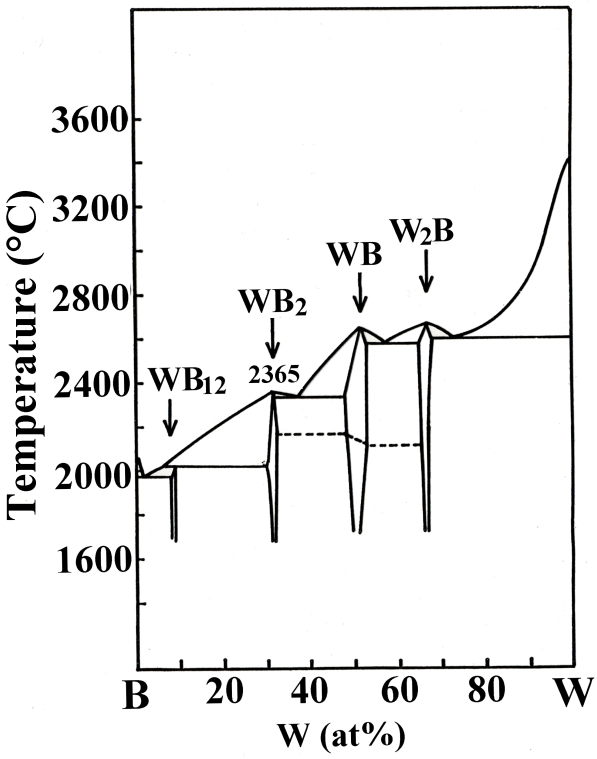

Figure 7. Binary W-B phase diagram [5].

C: B = 1 : $\sim$ 0.65 : $\sim$ 0.06, which makes the floating zone crystal growth much difficult than the cases of congruent melting compounds because crystal growth mode is not melt growth but has some similarity to flux growth. This crystal growth is often called "self flux growth". The difference between "flux growth" and "self flux growth" is ascribed to the difference of solute composition, i.e., under flux growth condition, WC content is $\sim$ 10 at% or less in metal flux such as Co, Ni and Fe, on the other hand, under self flux growth mode summation of W and C contents in the melt phase is more than 90 at%, thus it is called "self flux". The floating zone crystal growth under such self flux growth mode becomes much more difficult as compared with that under the congruent growth condition because any molten zone instabilities can cause a compositional instability of the molten zone, which can start depositing other than the WC phase. More technical details are available in ref. [6]. In addition to controlling the molten zone composition, feed rod of the WC crystal growth needs to have higher carbon and boron contents than crystal composition to compensate vaporization loss during the float zoning as shown in the top panel of figure 8 because C and B evaporate much faster than W at the growth temperature of $\sim$ 2700 °C. Note that the floating zone crystal growth of WC was performed using RF induction heating method as shown in figure 8 because the melting temperature is too high to achieve using even a Xenon-lamp image furnace.

An example of the obtained WC single crystal rod is shown in figure 9(a), where the zone passed through the rod from right to left, and the left end is the frozen molten zone. The vertical section shown in (b) indicates that the rod consists of the central single crystal region and the peripheral polycrystalline region. The back reflection Laue photograph perpendicular to the $(10\bar{1}0)$ shown in (c) indicates that the crystal has a rather good quality with no visible splitting of the Laue spots.

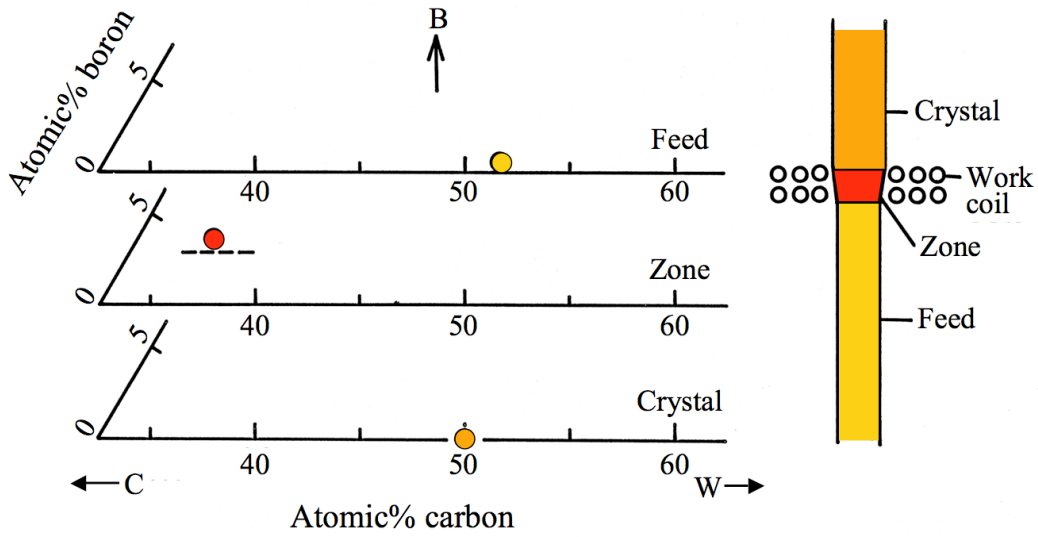

Figure 8. Compositions of the growing crystal, the molten zone and the feed rod plotted in the ternary W-B-C phase diagrams. The dotted line in the phase diagram for the molten zone indicates the lower limit of the boron content necessary to deposit the WC phase [6].

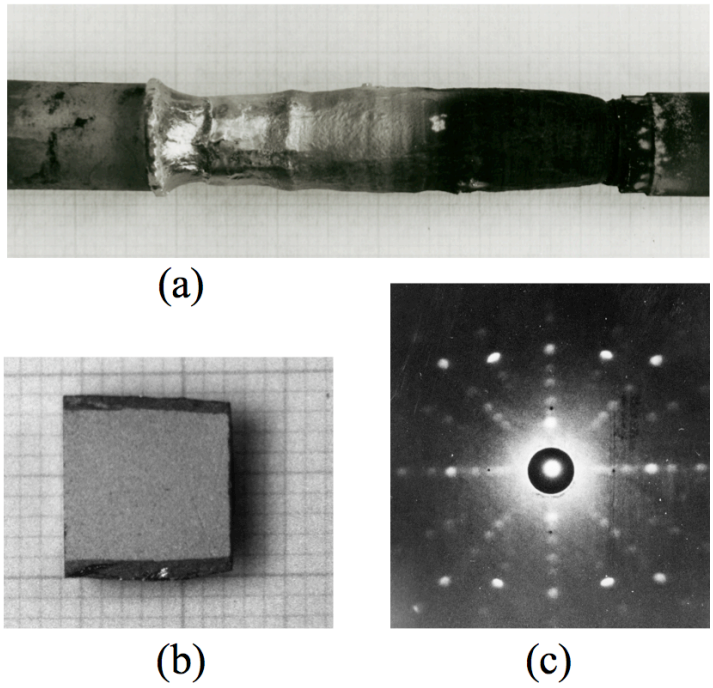

Figure 9. (a) An example of the floating zone grown single crystal of WC. (b) Vertical section of the rod. (c) Back reflection Laue photograph perpendicular to the $(10\bar{1}0)$ plane [6].

4. Boron icosahedron compounds

In metal-boron compounds bonding scheme of boron varies depending on the composition ratio [B]/[Me]. When the composition ratio exceeds 12, boron forms B_{12} icosahedron and three dimensional boron framework structure would be constructed by the linkage between the B_{12} icosahedra. There are many metal boron-icosahedron compounds, however, most of them decompose at high temperatures without melting. Their single crystals have been grown by high temperature solution growth method using metal flux such as Al, Cu, Sn etc. The obtained crystals were small because boron solubility in such flux metals are considerably low, which makes difficult to measure their physical properties.

Addition of an extra element should be considered to make floating zone method applicable to such decompositional boron-icosahedron compounds. According to the criterion presented in the previous section, C or Si can be a candidate for boron-icosahedron compounds. However, C has a tendency to increase melting temperature of borides, which is not suitable for the present purpose because the melting temperature should be decreased to the temperature region in which the target compound can stably exists. On the other hand, Si can reduce melting temperature of borides. In fact, the Si addition made floating zone crystal growth of some metal boron-icosahedron compounds possible. Those are YB_{50}, ScB_{19} and $ScB_{15}C_{0.8}$, which are described more in details.

4.1. YB_{50}

In binary Y-B system, five compounds of YB_2, YB_4, YB_6, YB_{12} and YB_{66} have been known to exist. During investigation of growing monochromator grade YB_{66} single crystals using floating zone method to develop a YB_{66} soft X-ray monochromator for dispersing synchrotron radiation in the energy range $1 \sim 2$ kev, we noticed that two unknown phases exist between YB_{12} and YB_{66}. Later we identified these 2 phases as YB_{25} [7] and YB_{50} [8]. Both compounds decompose at high temperatures without melting. The revised Y-B binary phase diagram is shown in figure 10. YB_{25} decomposes to YB_{12} and YB_{66} at ~ 1850 °C, meanwhile YB_{50} decomposes to YB_{25} and YB_{66} at ~ 1750 °C.

YB_{25} has a monoclinic crystal structure with space group either of $I121$ (No. 5), $I1m1$ (No. 8) and $I12/m1$ (No. 12) and lattice constants a=0.82842(3), b=1.03203(3) and c=0.58570(2) nm and β=90.402(3)°, which has a close structural similarity to $YAlB_{14}$. $YAlB_{14}$ has a $MgAlB_{14}$ type orthorhombic structure [9]. Deficit of Al site slightly distorts YB_{25} structure from orthorhombic to monoclinic [7].

We have initially identified YB_{50} to have an orthorhombic structure with space group $P21212$ and lattice constants a=1.66251(9), b=1.76198(11) and c=0.94797(3) nm. We have expected that YB_{50} has the same structure type as γ-AlB_{12} [10] because of the same space group and close similarities of lattice constants. Later we knew that the crystal structure of YB_{50} is completely different from that of γ-AlB_{12} and new.

A small amount of Si addition could make YB_{50} phase to stably coexist with a melt phase, which enabled us to grow single crystals of Si doped YB_{50} phase using floating zone method. On the other hand the YB_{25} phase vanished by the Si addition, i.e., YB_{25} phase has little Si solubility.

Floating zone crystal growth Floating zone crystal growth was carried out using an Xenon lamp image furnace as shown in figure 1. Several preliminary zone pass trials for feed rods with different compositions and chemical analyses of the zone passed rods and frozen molten zone indicated that the YB_{50} family compound with composition of approximately $YB_{45}Si_{1.0}$ can be grown from the melt of $YB_{40}Si_3$. Rods having nominal composition $YB_{45}Si_{1.8}$ were prepared by sintering green rods of raw YB_4, Si, and amorphous B powder mixture, where the difference

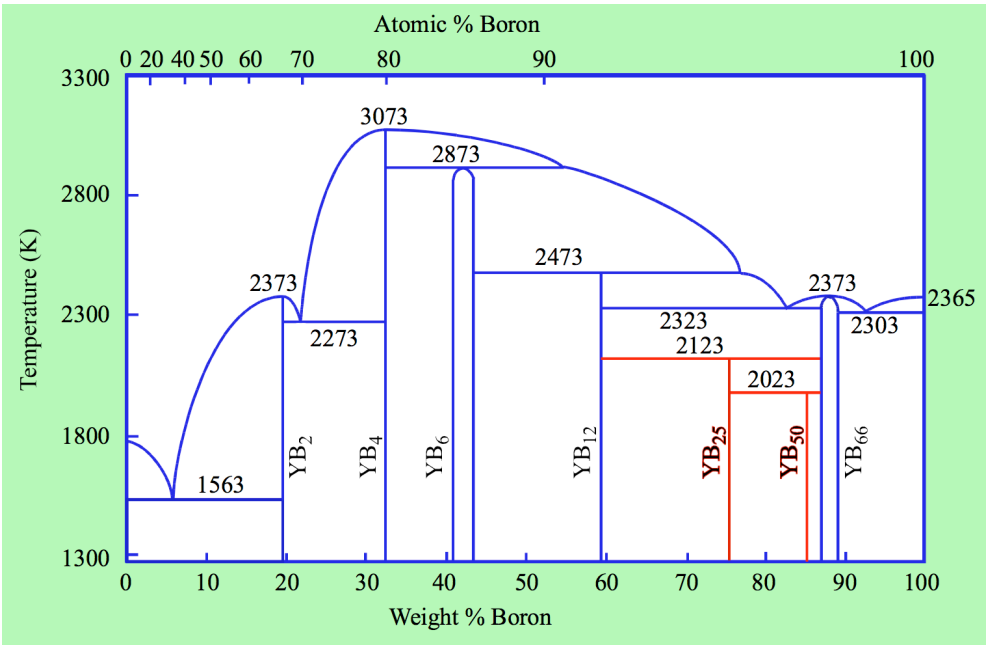

Figure 10. Y-B binary phase diagram

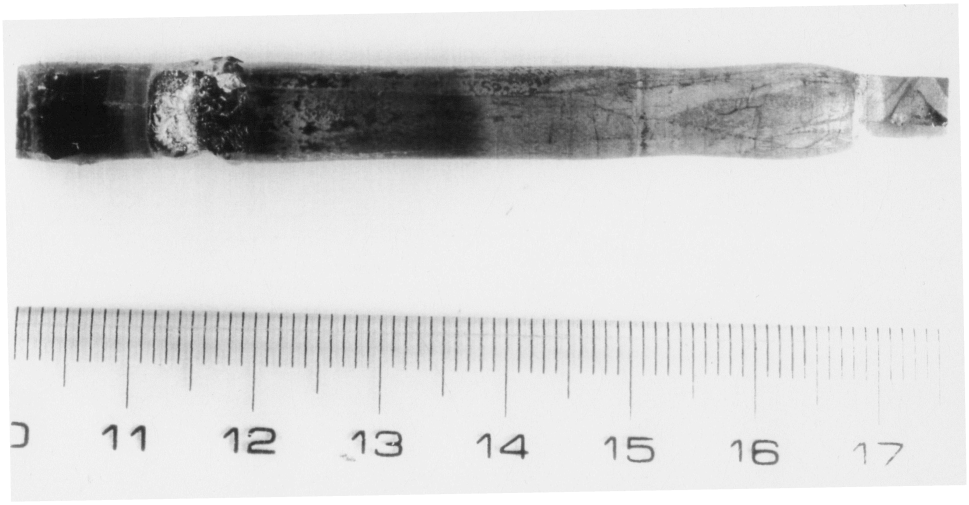

Figure 11. Single crystal of $YB_{44}Si_{1.0}$ [11].

between the nominal composition and the expected actual composition is due to the ignition loss during the sintering [11].

An example of the obtained single crystal is shown in figure 11.

X-ray diffraction pattern of the obtained $YB_{44}Si_{1.0}$ crystal is compared with that of YB_{50} synthesized by solid state reaction in figure 12. Both XRD patterns are quite similar except some minor differences such as slightly shorter lattice constants of $YB_{44}Si_{1.0}$ and intensity relation between diffraction peaks, which indicates both compounds have the same crystal structure. Structure analysis using the obtained $YB_{44}Si_{1.0}$ crystal revealed that $YB_{44}Si_{1.0}$ does not have

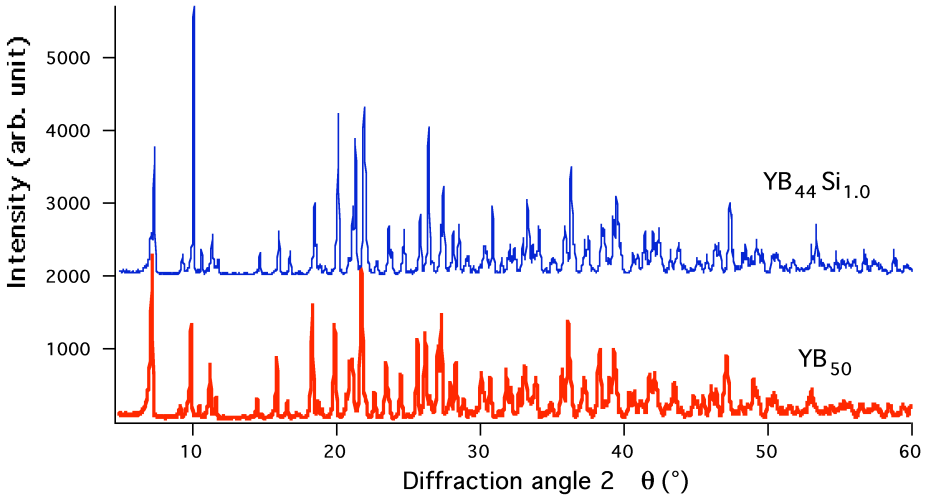

Figure 12. XRD patterns of single crystal of $YB_{44}Si_{1.0}$ and YB_{50} synthesized by solid state reaction [11].

γ-AlB_{12} type structure but has a new orthorhombic structure with space group Pbam. Details of the $YB_{44}Si_{1.0}$ structure is described in ref. [12], where chemical composition is described as $YB_{41}Si_{1.2}$ on the basis of single crystal X-ray structure analysis.

4.2. ScB_{19}

In binary Sc-B system, only two compounds of ScB_2 and ScB_{12} have been known to exist. Similar to the binary Y-B system case, we found ScB_{19} that decomposes at high temperatures without melting. The revised binary phase diagram is shown in figure 13.

ScB_{19} has a tetragonal crystal structure with space group either of $P41212$ or $P43212$ and lattice constants a, b=1.02915(4) nm and c=1.42463(9) nm [13], which has been expected to be isotypic to α-AlB_{12} because of similarities in cell dimensions and space group [14, 15].

Floating zone crystal growth Floating zone crystal growth was carried out using the same image furnace used for YB_{50} crystal growth. Feed rods for floating zone crystal growth were prepared by repeated horizontal zone-melting through rods that have prepared by sintering raw powders of $ScB_{17.5}$ and SiB_6 with a nominal composition $ScB_{19.9}Si_{0.4}$.

An example of the obtained crystals is shown in figure 14. X-ray diffraction pattern of the obtained $ScB_{19+x}Si_y$ is compared with that of ScB_{19} synthesized by solid state reaction in figure 15, where $ScB_{19+x}Si_y$ is used to the Si-doped ScB_{19} because the composition is variably dependent on the experimental conditions. Several extra peaks marked by an arrow in the XRD pattern of ScB_{19} are due to residual ScB_{27} (Sc-doped β-boron). It was confirmed that the grown $ScB_{19+x}Si_y$ and ScB_{19} are isostructural.

Table 1. Chemical compositions of the grown crystal shown in figure 13.

Position	Composition
Feed rod	$ScB_{17.8}Si_{0.17}$
Zone	$ScB_{12.4}Si_{1.90}$
Zone-end part crystal	$ScB_{18.0}Si_{0.22}$
Middle part crystal	$ScB_{19.2}Si_{0.27}$
Seed-end part crystal	$ScB_{19.0}Si_{0.27}$

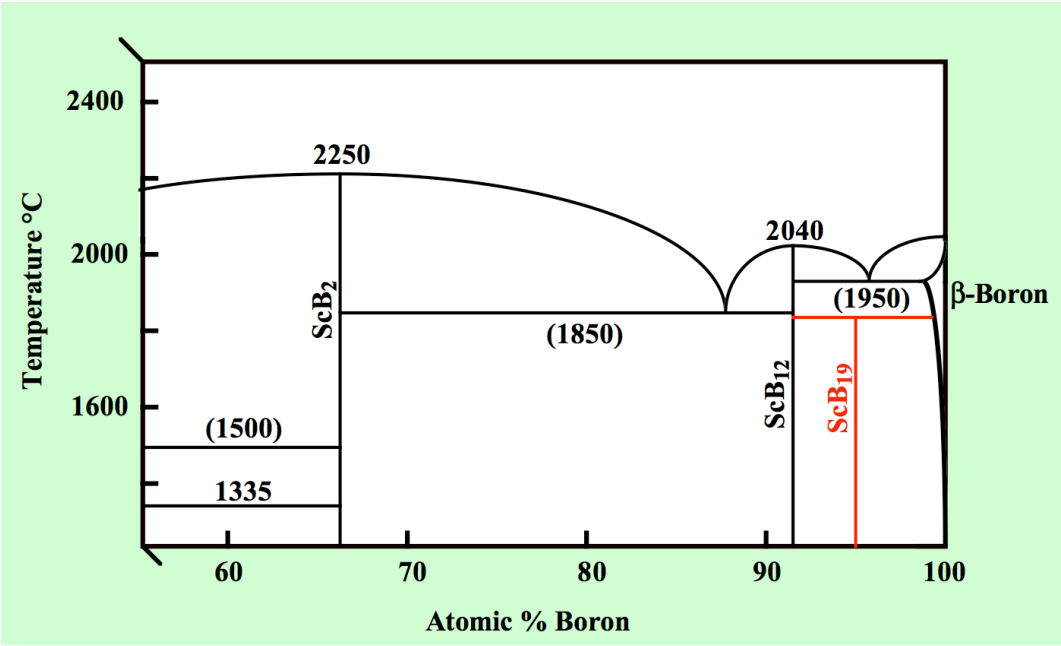

Figure 13. Sc-B binary phase diagram

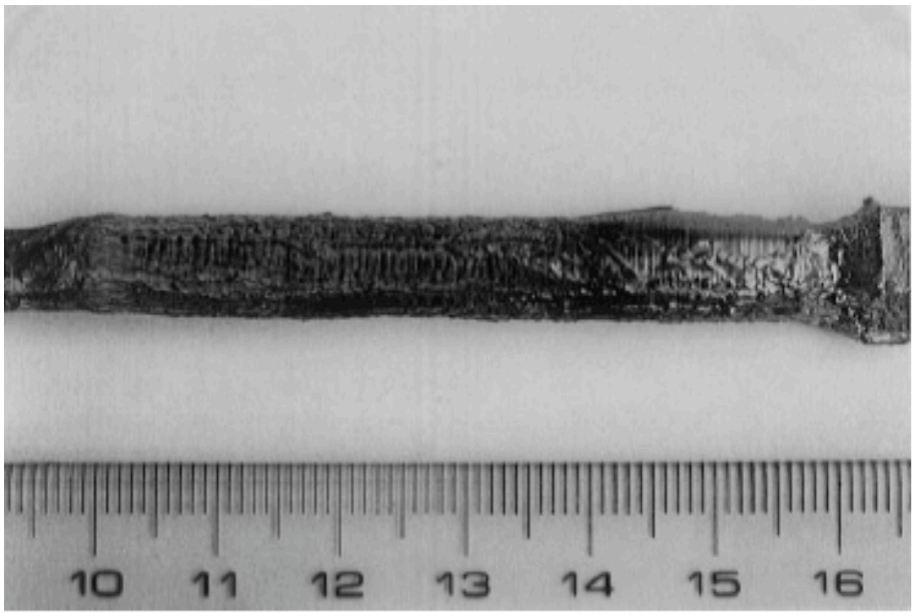

Figure 14. Single crystal of $ScB_{19+x}Si_y$ [16].

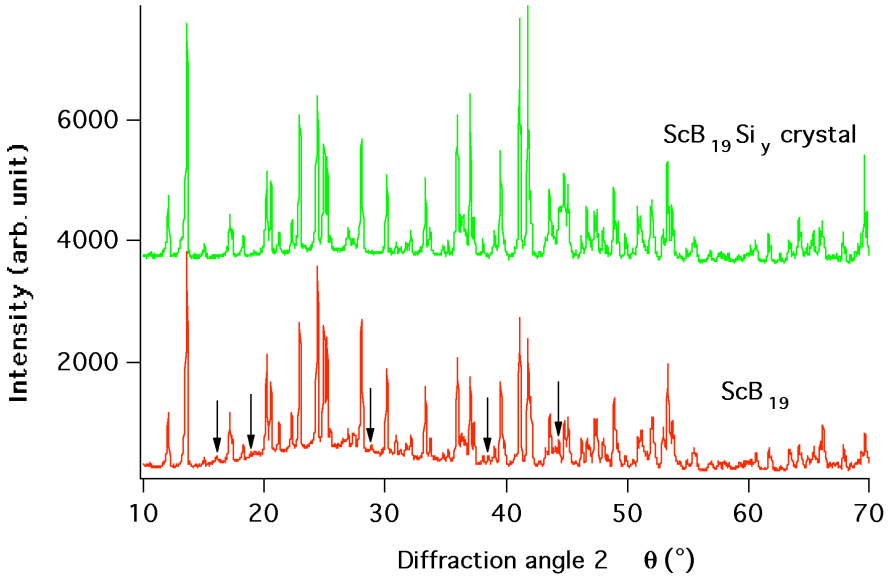

Figure 15. XRD patterns of single crystal $ScB_{19+x}Si_y$ and ScB_{19} synthesized by solid state reaction [16].

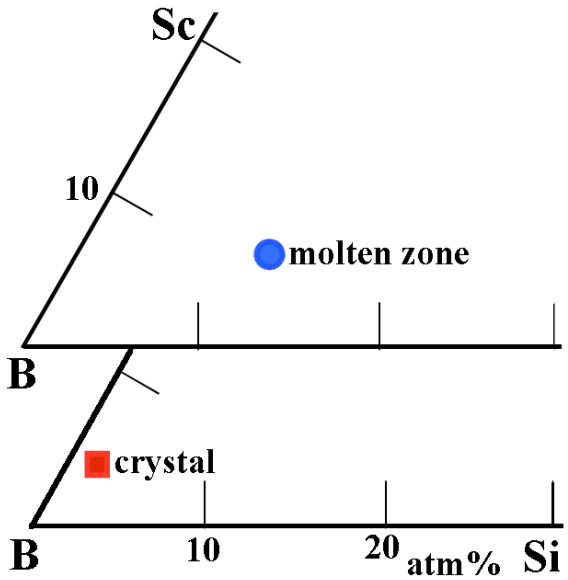

Figure 16. Compositions of the growing crystal and the molten zone in the boron-rich corner of the ternary Sc-B-Si phase diagrams.

Chemical compositions of the crystal shown in figure 14 are summarized in table 1. The molten zone composition whose Sc/B ratio is close to ScB_{12} is fairly less B and much Si as compared with that of the growing crystal. The composition relation between the growing crystal and the molten zone is illustrated in figure 16. The detail crystal structure of $ScB_{19+x}Si_y$ is described elsewhere [16].

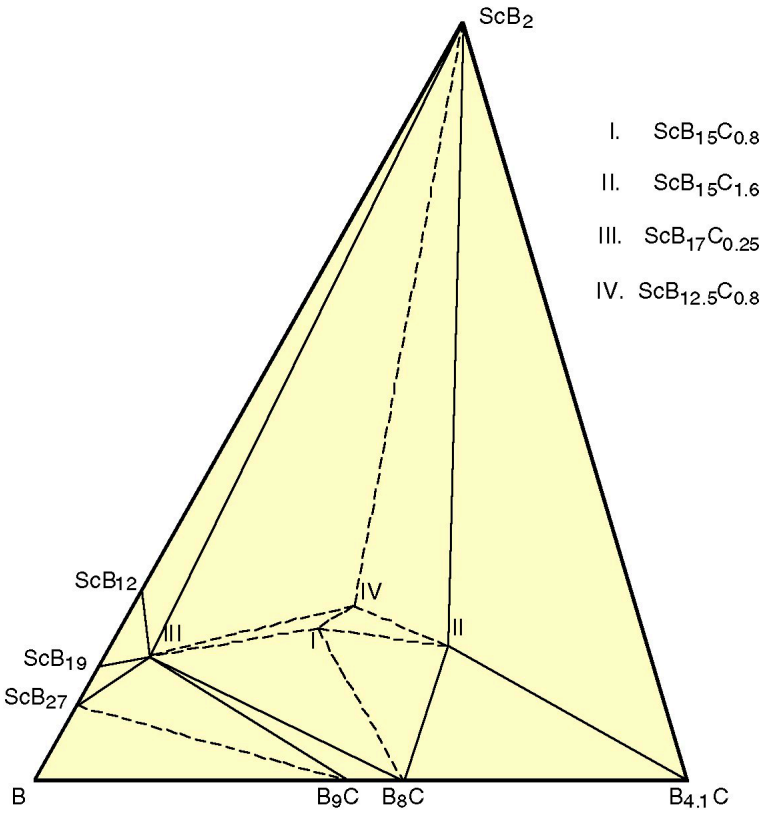

Figure 17. Boron-rich corner of the ternary Sc-B-C phase diagram.

4.3. $ScB_{15}C_{0.8}$

Figure 17 shows the boron-rich corner of the ternary Sc-B-C phase diagram obtained by solid state reaction. The solid state reaction could identify many boron-rich ternary Sc-B-C phases as indicated in the figure, except for $ScB_{12.5}C_{0.8}$ that parasitically appeared during floating zone crystal growth of Si-added $ScB_{15}C_{0.8}$. For most of them, we could determine their crystal structures; ScB_{19} [16], $ScB_{17}C_{0.25}$ [17, 18] and $ScB_{15}C_{1.5}$ [19]. However, X-ray diffraction pattern of the $ScB_{15}C_{0/8}$ prepared by solid state reaction was too complicated as shown in figure 18, which disenabled indexing the diffraction peaks, consequently its crystal structure has not been solved. Without any confidences that some of these phases can be grown by floating zone method with Si addition, we tried zone pass through a rod with composition of $\sim ScB_{15}C_{1.6}Si$.

Floating zone crystal growth Floating zone crystal growth was carried out using the same image furnace used for YB_{50} and ScB_{19} crystal growth. The first zone pass trial was carried out using a feed rod with a composition of $\sim ScB_{15}C_{1.6}Si_{1.0}$ expecting that an $ScB_{15}C_{1.6}$ phase crystal can be grown by the Si addition method. The zone pass was quite unstable and after only about 10 mm zone pass further zone pass became impossible. The obtained rod included so many small cracks and only the central region of about 2 mm diameter seemed to be a crystal. Powder XRD analysis for the central region indicated unexpectedly the existence of the $ScB_{15}C_{0.8}$ phase with some unknown phases. Thus, the second zone pass trial was carried out using a feed rod with a composition of $ScB_{15}C_{0.8}Si_{1.0}$. Stability of the zone pass was not so improved. When the molten zone was gradually cooled down after about 15 mm zone pass, its freezing behavior indicated the existence of excess free Si in it. For both the trials, the molten zone was formed by only

Figure 18. An example of $ScB_{15}C_{0.8}$ crystal [20].

melting the feed rod without adding an additional Si piece. The excess free Si in the molten zone after the rather short zone pass meant that the Si content in the feed rod was very high. By reducing the Si content in the feed rod by half of the second one the third zone pass trial could increase the central crystal region. Chemical analysis showed that the composition of the central crystal region was $ScB_{15.1}C_{0.89}Si_{0.22}$. Most of the powder XRD peaks could be assigned by a face-centered cubic structure with a lattice constant of a=2.0309 nm and an additional B_4C, which suggested that the real chemical composition of the cubic phase crystal should be less B and C than that of the feed rod. EPMA analysis for the crystal resulted a chemical composition of $\sim ScB_{12.5}C_{0.8}Si_{0.06}$. Single crystal structure analysis confirmed the chemical composition. An example of the grown crystals is shown in figure 18. Chemical analysis results of the crystal are summarized in table 2.

Table 2. Chemical compositions of the grown crystal shown in figure 18 [20].

Position	Composition
Feed rod	$ScB_{173.3}C_{0.65}Si_{0.066}$
Zone	$ScB_{9.9}C_{0.39}Si_{0.23}$
Zone-end part crystal	$ScB_{12.3}C_{0.57}Si_{0.071}$
Middle part crystal	$ScB_{12.3}C_{0.53}Si_{0.067}$
Seed-end part crystal	$ScB_{14.3}C_{0.78}Si_{0.104}$
Patition coefficients at the growth interface	
Element	*P. coefficient*
Si	$\sim$0.26
C	$\sim$1.2

X-ray diffraction pattern of the FZ-grown crystal is compared with that of the solid state reaction sample in figure 19. Both diffraction patterns show similarities, however, intensity relation of diffraction peaks are much different each other. This is probably due to lower Sc site occupancies of the solid state reaction sample as indicated by their chemical compositions.

More details of the floating zone crystal growth, structure analysis and crystal structure descriptions are reported in [20].

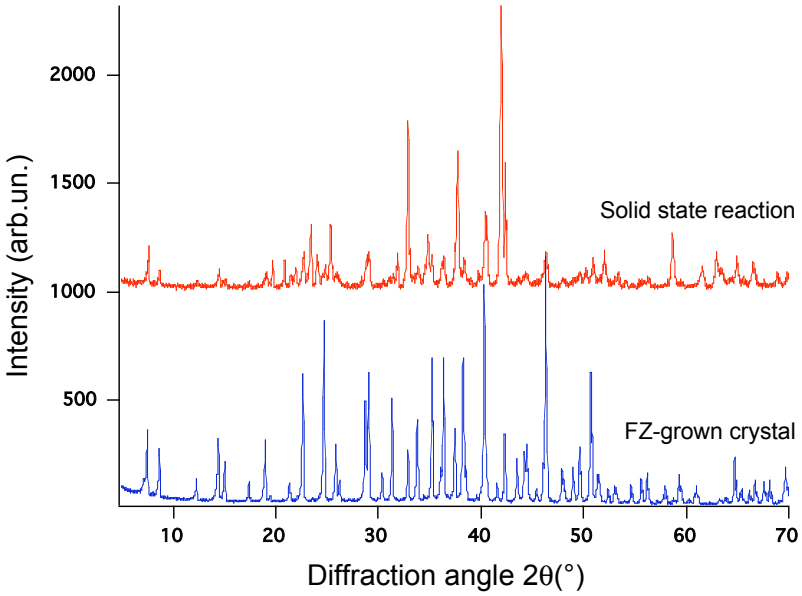

Figure 19. XRD patterns of FZ-grown single crystal $ScB_{12.7}C_{0.72}Si_{0.08}$ and $ScB_{15}C_{0.8}$ synthesized by solid state reaction.

5. Conclusion

Single crystal growth is very important for materials science. Newly found compounds need to be identified by structure analysis. The availability of single crystal of the compounds facilitates not only the identification but also investigation of physical properties of the compounds. Melt growth techniques such as Czochralski method, Bridgman method and zone melting method are powerful tool to obtain large size crystals, however, obviously those are not applicable to decomposition compounds. This manuscript describes that the addition of an extra element to the decomposition compound enables to apply melt growth method by modifying its phase behavior from decomposition to melting. For WC boron addition was effective to modify its melting behavior and large single crystals could be grown by floating zone method. The Si addition to the rare-earth boron icosahedron compounds was not only effective to modify its melting behavior but also revealed the existence of some Sc boron icosahedron compounds [21, 22]. The author hopes that this manuscript helps readers to understand the concept of the addition of an extra element to the decomposition compounds to modify its phase behavior and to facilitate melt crystal growth, and give them incentive to apply the concept to their crystal growth investigation.

References

[1] Rudy E 1973 *J. Less-Common Metals* **33** 245
[2] Sara R V 1965 *J. Am. Ceram. Soc.* **48** 25

[3] Okamoto H 1990 *C-W (Carbon-Tungsten), Binary Alloy Phase Diagrams* 2nd ed. (ed) T B Massalski p 895
[4] Demetriou M D, Ghonien N M and Lavine A S 2002 *J. Phase Equilib.* **23** 305
[5] Rudy E 1969 *AFML-TR-65-2, Part V "Compendium of Phase Diagram Data"* (A.F. Matrials Lab.; WRIGHT-PATTERSON AFB) p. 214
[6] Tanaka T, Otani S and Ishizawa Y 1988 *J. Mater. Sci.* **23** 665
[7] Tanaka T, Okada S, Yu Y and Ishizawa Y 1997 *J. Solid State Chem.* **133** 122
[8] Tanaka T, Okada S and Ishizawa Y 1994 *J. Alloys Compd.* **205** 281
[9] Korsukova M M, Lundström T, Tregenius L-E and Gurin V N 1992 *J. Alloys bf 187* 39
[10] Higashi I 1983 *J. Solid State Chem.* **47** 333
[11] Tanaka T, Okada S and Ishizawa Y 1997 *J. Solid State Chem.* **133** 55
[12] Higashi I, Tanaka T, Kobayashi K, Ishizawa Y and Takami M 1997 *J. Solid State Chem.* **133** 11
[13] Tanaka T, Okada S and Ishizawa Y 1998 *J. Alloys Compd.* **267** 211
[14] Higashi I, Sakurai T and Atoda T 1977 *J. Solid State Chem.* **20** 67
[15] Kasper J S, Vlasse M and Naslain R 1977 *J. Solid State Chem.* **20** 281
[16] Tanaka T and Sato A 2001 *J. Solid State Chem.* **160** 394
[17] Tanaka T 1998 *J. Alloys Compd.* **270** 132
[18] Leithe-Jasper A, Sato A and Tanaka T 2000 *J. Solid State Chem.* **154** 130
[19] Leith-Jasper A, Sato A and Tanaka T 2000 *Z. Kristalogr.* NCS **216** 45
[20] Tanaka T and Sato A 2002 *J. Solid State Chem.* **165** 148
[21] Tanaka T, Yamamoto A and Sato A 2002 *J. Solid State Chem.* **168** 192
[22] Tanaka T, Yamamoto A and Sato A 2004 *J. Solid State Chem.* **177** 476